δ18O water isotope in the iLOVECLIM model (version 1.0) – Part 3: A palaeo-perspective based on present-day data–model comparison for oxygen stable isotopes in carbonates

T. Caley, Didier M. Roche

Geosci. Model Dev., 6, 1505–1516, 2013
www.geosci-model-dev.net/6/1505/2013/
doi:10.5194/gmd-6-1505-2013

Geoscientific Model Development
Open Access

δ^{18}O water isotope in the *i*LOVECLIM model (version 1.0) – Part 3: A palaeo-perspective based on present-day data–model comparison for oxygen stable isotopes in carbonates

T. Caley[1] **and D. M. Roche**[1,2]

[1]Earth and Climate Cluster, Faculty of Earth and Life Sciences, Vrije Universiteit Amsterdam, Amsterdam, the Netherlands
[2]Laboratoire des Sciences du Climat et de l'Environnement (LSCE), UMR8212, CEA/CNRS-INSU/UVSQ, Gif-sur-Yvette Cedex, France

Correspondence to: T. Caley (t.caley@vu.nl)

Received: 5 February 2013 – Published in Geosci. Model Dev. Discuss.: 4 March 2013
Revised: 24 July 2013 – Accepted: 31 July 2013 – Published: 12 September 2013

Abstract. Oxygen stable isotopes (δ^{18}O) are among the most useful tools in palaeoclimatology/palaeoceanography. Simulation of oxygen stable isotopes allows testing how the past variability of these isotopes in water can be interpreted. By modelling the proxy directly in the model, the results can also be directly compared with the data. Water isotopes have been implemented in the global three-dimensional model of intermediate complexity *i*LOVECLIM, allowing fully coupled atmosphere–ocean simulations. In this study, we present the validation of the model results for present-day climate against the global database for oxygen stable isotopes in carbonates. The limitation of the model together with the processes operating in the natural environment reveal the complexity of use the continental calcite-δ^{18}O signal of speleothems for a global quantitative data–model comparison exercise. On the contrary, the reconstructed surface ocean calcite-δ^{18}O signal in *i*LOVECLIM does show a very good agreement with the late Holocene database (foraminifers) at the global and regional scales. Our results indicate that temperature and the isotopic composition of the seawater are the main control on the fossil-δ^{18}O signal recorded in foraminifer shells when all species are grouped together. Depth habitat, seasonality and other ecological effects play a more significant role when individual species are considered. We argue that a data–model comparison for surface ocean calcite δ^{18}O in past climates, such as the Last Glacial Maximum ($\approx$ 21 000 yr), could constitute an interesting tool for mapping the potential shifts of the frontal systems and circulation changes throughout time. Similarly, the potential changes in intermediate oceanic circulation systems in the past could be documented by a data (benthic foraminifers)-model comparison exercise whereas future investigations are necessary in order to quantitatively compare the results with data for the deep ocean.

1 Introduction

Water isotopes are commonly used as important tracers of the hydrological cycle. Because of small chemical and physical differences between the main isotopic forms of the water molecule ($H_2{}^{16}O$, HDO, $H_2{}^{18}O$), an isotopic fractionation occurs, principally during phase transitions of water (evaporation and condensation processes). Stable water isotopes have therefore been measured in a large variety of archives to reconstruct regional climate variations. In polar ice cores, the isotopic composition of the ice has long been used to reconstruct past air temperatures (Dansgaard, 1953; Jouzel, 2003; Jouzel et al., 2007). For tropical ice cores (Thompson et al., 2000), temperature but also precipitation intensity upstream of the air mass trajectories seems to play an important role to explain water isotope signals (Hoffmann et al., 2003; Vimeux et al., 2005). Over the continent, water isotope concentration is preserved in carbonate from speleothems or lacustrine organism such as ostracodes, reflecting the isotopic composition of meteoric water and the temperature dependent water–calcite oxygen isotope fractionation (Urey, 1947; Kim and O'Neil, 1997). For speleothems in tropical regions,

some studies have suggested that the amount of precipitation, called amount effect, (Dansgaard, 1964; Rozanski et al., 1993) could be the dominant driver of water isotope concentration (Burns et al., 2002; Fleitmann et al., 2003; Wang et al., 2001). In lakes, water isotope composition can be dependant on temperature, air mass source area and/or a precipitation / evaporation ratio (Stuiver, 1970; Leng and Marshall, 2004).

Similarly to palaeocontinental archives, the seawater oxygen isotope concentration ($\delta^{18}O_{sw}$) is preserved in carbonates from various organisms such as foraminifers and corals. The carbonate isotopic concentration is mainly controlled by temperature and by the isotopic composition of seawater during their formation (Urey, 1947; Shackleton, 1974).

If water isotopes are one of the most widely used proxies in climate archives from the different realms, processes that control their compositions are various and complex. Models allow testing how the past variability of isotopes in water can be interpreted. For example, the importance of temperature versus precipitation changes for the climatic interpretations of tropical isotopic records (Risi et al., 2010). Models can also help to determine the validity of using modern spatial gradients to derive temporal gradients, i.e. the covariability of climate and water isotopes in a specific location over time (Schmidt et al., 2007; Legrande and Schmidt, 2009). By modelling the proxy (water isotopes) directly in the model, the results can also be directly compared with the data. In addition, simulation of climate and its associated isotopic signal can provide a "transfer function" between isotopic signal and the considered climate variable (Sturm et al., 2010).

General circulation models (GCMs) have been frequently used for isotopic studies (Jouzel et al., 1987; Joussame and Jouzel, 1993; Hoffmann et al., 1998; Schmidt, 1998; Delaygue et al., 2000; Paul et al., 1999; Noone and Simmonds, 2002; Mathieu et al., 2002; Lee et al., 2007; Schmidt et al., 2007; Yoshimura et al., 2008; Zhou et al., 2008; Tindall et al., 2009; Risi et al., 2010; LeGrande and Schmidt, 2011; Werner et al., 2011; Xu et al., 2012). Among them, the majority has been used exclusively to simulate water isotopes separately in the atmosphere and ocean components. Oxygen isotopes have been implemented in the three-dimensional model of intermediate complexity called *i*LOVECLIM (version 1.0), allowing fully coupled atmosphere–ocean simulations. The detailed implementations of oxygen isotopes in *i*LOVECLIM can be found in Roche (2013). The present work aims at showing preindustrial experiment results in comparison to different global datasets from marine and continental realms. We mainly focus our discussion on carbonate archives that are extensively used in climate studies. The validation of the model results against water isotope observations can be found in Roche and Caley (2013). The benefits, caveats, agreements and problems from this data–model comparison for oxygen stable isotopes in carbonates will be discussed to determine the potential and the interest of using *i*LOVECLIM for palaeoclimatic studies.

2 Method

2.1 Water isotopes definition, notation and fractionation

Isotopic values are measured by a mass spectrometer and expressed relative to a standard as (δ) notations (Sharp, 2007):

$$\delta^{18}O = R(^{18}O)_P / R(^{18}O)_{std} - 1,$$

R is the abundance ratio of the heavy and light isotopes (e.g. $N(^{18}O)_p/N(^{16}O)_P$) for substance P and δ is commonly reported in units of parts per thousand (‰). The standard for carbonate is Pee Dee Belemnite (PDB) (Craig, 1957) and that for waters is standard mean ocean water (SMOW) (Baertschi, 1976). More recently, standards have been defined with the prefix "Vienna" or VSMOW and VPDB to account for the exhaustion of the original standard materials (Coplen, 1996).

The magnitude of fractionation can be expressed on the δ scale through the logarithmic transformation $10^3\ln(\alpha_{A-B})$ where $\alpha_{A-B} = R_A/R_B$, α is the equilibrium fractionation and R is the partitioning of isotopes between two substances or two phases of the same substance A and B.

2.2 Oxygen isotopes in *i*LOVECLIM

The *i*LOVECLIM (version 1.0) model is a derivative of the LOVECLIM-1.2 climate model extensively described in Goosse et al. (2010). With regards to water isotopes, the main development lies in the atmospheric component in which evaporation, condensation and existence of different phases (liquid and solid) all affect the isotopic conditions of the water isotopes. In the ocean, the water isotopes are acting as passive tracers ignoring the small fractionation implied by the presence of sea ice (Craig and Gordon, 1965). For the land surface model, the implementation in the bucket follows the same procedure as for the water except that equilibrium fractionation is assumed during phase changes. A detailed description of the method used to compute the water isotopes in *i*LOVECLIM can be found in Roche (2013).

2.3 Global datasets

Global oxygen isotopic datasets for the atmosphere and ocean components have been compiled from published late Holocene measurements to allow comparison and discussion with *i*LOVECLIM results. Table S1 is a compilation of 74 δ^{18}O calcite measurements and drip water data of speleothems from the literature. The δ^{18}O of the calcite are reported for the last 1000 years of each record with the associated 2σ error when it was possible to calculate it. Table S1 also includes a compilation of 19 δ^{18}O data of ice

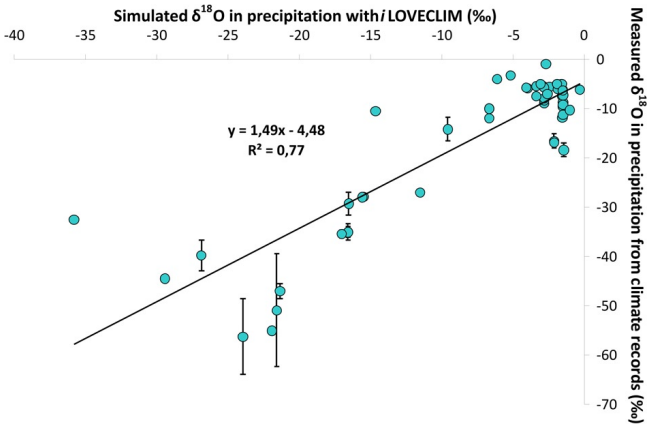

Fig. 1. Simulated δ^{18}O in precipitation with *i*LOVECLIM in comparison to measured δ^{18}O in precipitation from climate records (speleothems drip water and ice cores) (Table S1).

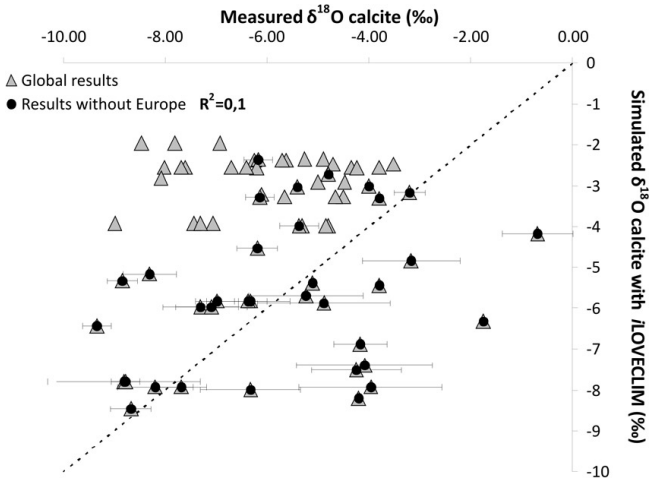

Fig. 2. Simulated calcite-δ^{18}O values based on δ^{18}O in precipitation and atmospheric temperature from *i*LOVECLIM results (using Kim and O'Neil, 1997 equation) in comparison to measured calcite δ^{18}O of late Holocene speleothem records (Table S1).

cores from the literature. The δ^{18}O of the ice are reported for the last 1000 yr of each record with the associated 2σ error when it was possible to calculate it. For the EPICA Dome C, Vostok and Illimani site, the δD values were converted in δ^{18}O values using the global meteoric water line $\delta\mathrm{D} = 8.2 \times \delta^{18}\mathrm{O} + 11.27$ (Rozanski et al., 1993). To compare global oceanic isotopic datasets with *i*LOVECLIM results, we used the late Holocene planktonic foraminifer's δ^{18}O database of Waelbroeck et al. (2005) and extend it with 62 data averaging over the last 3000 yr (Table S2). Similarly, for the intermediate and deep ocean, we used the published Atlantic benthic foraminifer's stable isotopic database of Marchal and Curry (2008) and extend it with 73 data covering the global ocean and averaged over the last 3000 yr (Table S2).

3 Results and discussion

3.1 Oxygen isotopes: from the atmosphere to continental records

The water evaporated from the surface ocean undergoes a poleward transport over landmasses that results in gradual rainout and a depletion of the remaining moisture in ^{18}O. The δ^{18}O in precipitation shows therefore systematic variations with latitude, altitude and distance from vapour source. The δ^{18}O in precipitation can then be conserved in continental carbonate archives. Under equilibrium conditions, the δ^{18}O of carbonates (speleothem) depends on both the temperature through its control on equilibrium fractionation between water and calcite (Hendy, 1971; Kim and O'Neil, 1997) and the isotopic composition of the drip water from the cave site in which the speleothem grew. Using the Kim and O'Neil (1997) equation for synthetic calcite and making the approximation that $1000 \times \ln\alpha(\text{calcite-water}) \approx \delta\text{calcite-}\delta\text{water}$, it can be demonstrated that $\delta^{18}\mathrm{O}$ calcite(speleothem) $= \delta^{18}\mathrm{O}$ water$+(18.03 \times (1000/T) - 32.17)$. T is the temperature in Kelvin and the relationship between the two scales (PDB and SMOW) can be expressed as $\delta^{18}\mathrm{O(PDB)} = 0.97002(\delta^{18}\mathrm{O(SMOW)}) - 29.98$ (Coplen et al., 1983; Sharp, 2007).

Figure 1 shows the results obtained with *i*LOVECLIM for the present-day δ^{18}O in precipitation in comparison to drip water data from spelothems and ice core data (Table 1). The observed relationship is good ($R^2 = 0.77$). This confirms that the model is capable of representing the global distribution of δ^{18}O in precipitation as demonstrated in Roche and Caley (2013), although an underestimation of the fractionation towards lower temperatures/latitudes is observed (Roche and Caley, 2013).

Combining the δ^{18}O of precipitation and atmospheric temperature and using the equation of Kim and O'Neil (1997), we are able to reconstruct the calcite δ^{18}O in the model and to compare it with late Holocene calcite-δ^{18}O data (Fig. 2 and Table S1).

We conducted this analysis separately for the European region and for the rest of the world. Indeed, the interpretation of the δ^{18}O in precipitation signal over Europe has been found to be complex in *i*LOVECLIM, probably linked to the representation of the Mediterranean region in the model (Roche and Caley, 2013). Nonetheless, a discrepancy between model results and data exist also when the Europe area is excluded (Fig. 2). An insignificant correlation ($R^2 = 0.1$) can be observed between measured calcite-δ^{18}O and model results (Fig. 2). This weak relationship can be explained by a combination of factors. First, the representation of the δ^{18}O in precipitation with the model. In particular the low resolution and simple representation of the atmospheric component

Table 1. Data–model comparison for the calcite-δ^{18}O signal of individual foraminiferal species using various palaeotemperature equations (Shackleton, 1974 and Mulitza et al., 2003). Note that for the depth habitat, they have been estimated based on calcification depth found in the literature (Ottens, 1992; Kohfeld et al., 1996; Bauch, 1997; Bauch et al., 2002; Ganssen and Kroon, 2000; Ostermann et al., 2001; Pak and Kennett, 2002; Anand et al., 2003; Simstich, 2003; Pak et al., 2004; Kuroyangi and Kawahata, 2004; von Langen et al., 2005; Came et al., 2007; Farmer et al., 2007). However, foraminifera are not restricted to a certain depth level and can change their habitat depth with time or at specific locations (Waelbroeck et al., 2005).

Foraminiferal species	Depth habitat estimation (m)	Palaeotemperature equation by Shackleton (1974)	Data–model R^2	Palaeotemperature equations by Mulitza et al. (2003)	Data–model R^2
G. ruber white	0–50	$T = 16.9 - 4.38(\delta c - \delta w) + 0.1(\delta c - \delta w)2$	0.76	$T = -4.44(\delta c - \delta w) + 14.20$	0.76
G. ruber pink	0–25	$T = 16.9 - 4.38(\delta c - \delta w) + 0.1(\delta c - \delta w)2$	0.51	$T = -4.44(\delta c - \delta w) + 14.20$*	0.51
G. sacculifer	0–50	$T = 16.9 - 4.38(\delta c - \delta w) + 0.1(\delta c - \delta w)2$	0.63	$T = -4.35(\delta c - \delta w) + 14.91$	0.63
G. bulloides	0–50	$T = 16.9 - 4.38(\delta c - \delta w) + 0.1(\delta c - \delta w)2$	0.73	$T = -4.70(\delta c - \delta w) + 14.62$	0.72
N. Pachyderma dextral	0–75	$T = 16.9 - 4.38(\delta c - \delta w) + 0.1(\delta c - \delta w)2$	0.5	$T = -3.55(\delta c - \delta w) + 12.69$	0.48
N. Pachyderma sinistral	0–150	$T = 16.9 - 4.38(\delta c - \delta w) + 0.1(\delta c - \delta w)2$	0.11	$T = -3.55(\delta c - \delta w) + 12.69$	0.11

that complicates certain aspects of the data–model comparison (Roche and Caley, 2013). Second, the altitudinal effect and its impact on the δ^{18}O in precipitation (around -2.5 ‰/1000 m; Lachniet, 2009) is not fully taken into account in different areas due low resolution of the atmospheric model preventing high elevations in mountain ranges (e.g. the Alps are $\approx$ 1200 m in height). Nonetheless a correction of this altitudinal effect does not significantly change the results of the correlation for our global database (not shown). Another factor is the use of atmospheric temperatures rather than cave temperatures in the calcite-δ^{18}O calculation with the modelling results. Indeed, the relationship between measured temperature in the cave and atmospheric temperature in the model is significant but weak ($R^2 = 0.63$, Fig. 3). Taken together, all these limitations lead to a bias of the calcite δ^{18}O reconstructed when using the model results. Another source of uncertainties of this data–model comparison correspond to all potential biases which occur in the natural environment, processes operating in the atmosphere, soil zone, epikarst and cave system (Lachniet, 2009) and affecting the measured calcite-δ^{18}O signal (Fig. 2). For example, recent studies suggest the precipitation of the calcite in different caves does not occur under equilibrium conditions indicating significant kinetic isotope effects during speleothem calcite growth (Mickler et al., 2006; Daëron et al., 2011). This is an important limitation for a global quantitative comparison between model and data.

For a better representation at the local scale of the calcite-δ^{18}O signal in tropical and mid-latitude region, models with higher complexity and resolution are necessary (Wackerbarth et al., 2012). Furthermore, more processes operating between the atmosphere and the cave system need to be integrated, in addition to the knowledge of the isotopic composition of precipitation and temperature, to allow a good quantitative reconstruction of the calcite-δ^{18}O signal. It remains to be tested if qualitative data – model comparison for the calcite-δ^{18}O signal (i.e. anomaly between the past and present day) would give better results with our model.

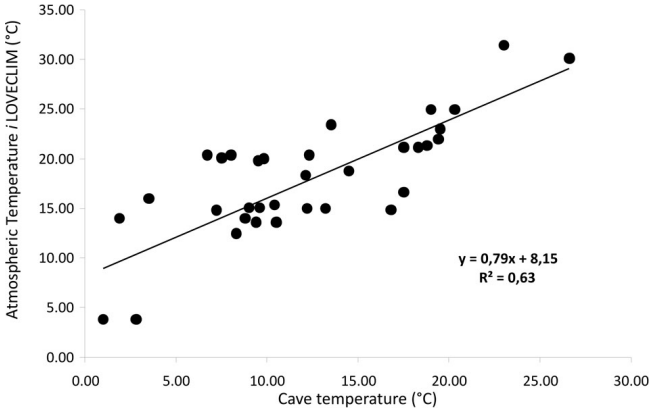

Fig. 3. Relationship between atmospheric (*i*LOVECLIM results) and cave temperature (Table S1).

Another possibility is to use the method recently developed to extract the fossil water of speleothem record (Vonhof et al., 2006; van Breukelen et al., 2008). With this water, it becomes possible to reconstruct hydrogen and oxygen stable isotope analyses of fossil precipitation. Based on our work, it appears that reconstructed fossil water isotopic signals may allow a better quantitative comparison with modelling results (Fig. 1). The signal would also be more easily related to tropical precipitation (Roche and Caley, 2013) than the complex calcite-δ^{18}O signal.

3.2 Oxygen isotopes: from the ocean to the foraminifer shells

The seawater oxygen isotope concentration ($\delta^{18}O_{sw}$) tracks regional freshwater sources (evaporation, precipitation and river input) and water mass exchange through surface ocean fluxes and ocean circulation (Jacobs et al., 1985; Skinner et al., 2003). It yields information on changes in the hydrological cycle in the past. The $\delta^{18}O_{sw}$ is preserved in ocean carbonate archives as foraminifer shells. δ^{18}O of foraminifer

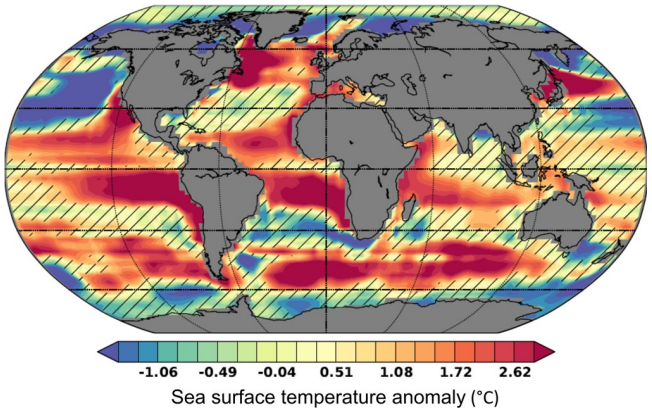

Fig. 4. Anomaly of mean sea surface temperature (modelled in *i*LOVECLIM – Levitus and Boyer, 1994). The hatching denotes areas where the difference is less than 1 °C.

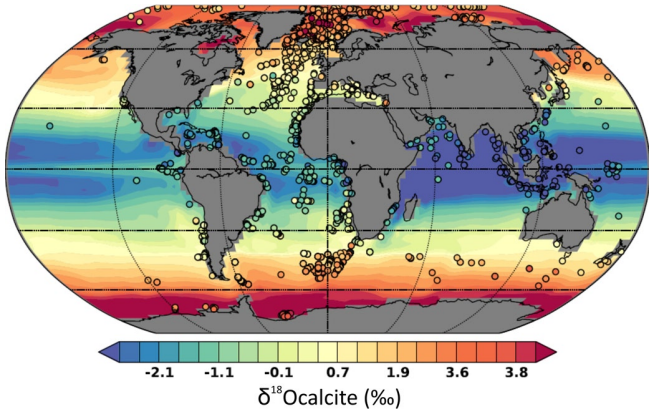

Fig. 5. Simulated ocean calcite δ^{18}O (0–50 m) for the present day with *i*LOVECLIM. Superimposed dots represent calcite-δ^{18}O data measured on the various shallowest dwelling foraminifer species (Waelbroeck et al., 2005, extended by 62 points: Table S2). Note that the legend is non-linear.

calcite is mainly controlled by temperature and by the isotopic composition of seawater in which the shell grew (Urey, 1947; Shackleton, 1974). The temperature dependence of the equilibrium fractionation of inorganic calcite precipitation around 16.9 °C is given in Shackleton (1974) as

$$T = 16.9 - 4.38(\delta^{18}O_{carbonate(PDB)} - \delta^{18}O_{sw(SMOW)}) + 0.1(\delta^{18}O_{carbonate(PDB)} - \delta^{18}O_{sw(SMOW)})^2.$$

Mathematically we can write the inverse equation for the δ^{18}O of the water:

$$\delta^{18}O_{sw(SMOW)} = \delta^{18}O_{carbonate(PDB)} + 0.27 - 21.9 + \sqrt{(310.6 + 10\,T)}.$$

The conversion between the two scale (PDB and SMOW) can be expressed as δ^{18}O water(VPDB) = δ^{18}O water(VSMOW))−0.27 (Hut, 1987).

3.2.1 Surface ocean

Because the calcite δ^{18}O depends on temperature and $\delta^{18}O_{sw}$, the modelled two parameters must be assessed. The $\delta^{18}O_{sw}$ results of the model were evaluated against δ^{18}O in water samples in Roche and Caley (2013), and the agreement is found to be very good. We compare the Levitus and Boyer (1994) data and model results to assess the modelled temperature. From this comparison it appears that sea surface temperature (SST) in the model are in good agreement with data (overall, less than 1 °C of differences is observed) (Fig. 4) and therefore cannot lead to important bias on the calcite-δ^{18}O signal. We focus on regions where SSTs are significantly warmer or colder in the model in comparison to data and where some notable discrepancies between the modelled distribution and data for the $\delta^{18}O_{sw}$ have been observed (Roche and Caley, 2013).

The main differences for the $\delta^{18}O_{sw}$ are in the Atlantic and Indian subtropical Ocean and the region offshore from California (Roche and Caley, 2013). These regions are all marked by warmer SST in the model (Fig. 4). The $\delta^{18}O_{sw}$ in the model is slightly depleted in the Atlantic Ocean and even more depleted in the North Indian Ocean in comparison to data (Roche and Caley, 2013). These two effects (warmer SST and more depleted $\delta^{18}O_{sw}$) produce both a weak supplementary decrease of the δ^{18}O calcite signal but no compensation effect. Concerning the region offshore from California, the warmer SST and more enriched $\delta^{18}O_{sw}$ could compensate each other but the modelled signal is compared to only two calcite-δ^{18}O points of our dataset (Fig. 5). Therefore, the δ^{18}O calcite signal of the model can be compared with data with a good accuracy because slight errors in the modelled temperature and water isotope distributions do not compensate each other. Also note that the problem of biased absolute SST values may not apply when anomalies with respect to past climates are calculated (for example the last glacial maximum).

Combining the $\delta^{18}O_{sw}$ and oceanic temperature and using the equation of Shackleton (1974), we are able to reconstruct the calcite δ^{18}O in the model and to compare it with late Holocene δ^{18}O planktonic foraminifers' data (Fig. 5). We choose specifically the interval 0–50 m as the different species of foraminifers that constitute the global dataset (*G. Ruber pink*, *G. Ruber white*, *G. sacculifer*, *G. bulloides*, *N. Pachyderma dextral and sinistral*) have various depth habitats but they are all among the shallowest dwelling species. Indeed, the depth habitat for *G. Ruber pink* is 0–25 m (Ganssen and Kroon, 2000; Anand et al., 2003; Farmer et al., 2007), 0–50 m for *G. Ruber white* (Ganssen and Kroon, 2000; Anand et al., 2003; Farmer et al., 2007), 0–50 m for *G. sacculifer* (Ganssen and Kroon, 2000; Anand et al., 2003; Farmer et al., 2007), 0–50 m for *G. bulloides* (Ganssen and Kroon, 2000; Pak et al., 2004), 0–75 m for *N. Pachyderma*

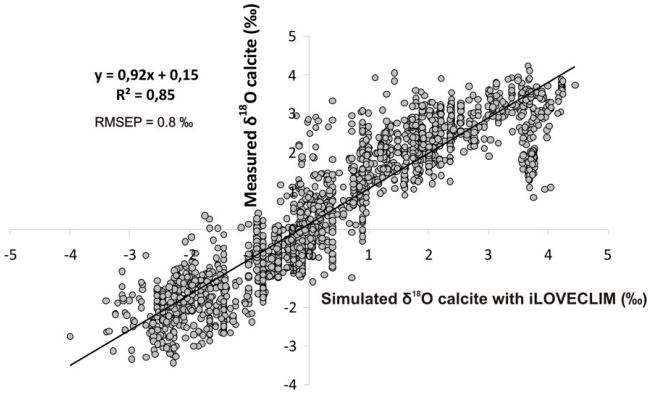

Fig. 6. Relationship between the ocean calcite δ^{18}O calculated in the model (0–50 m depth) and calcite-δ^{18}O measurements on the various shallowest dwelling foraminifer species (Waelbroeck et al., 2005 with $1\sigma < 0.3$ ‰, extended by 62 points: Table S2).

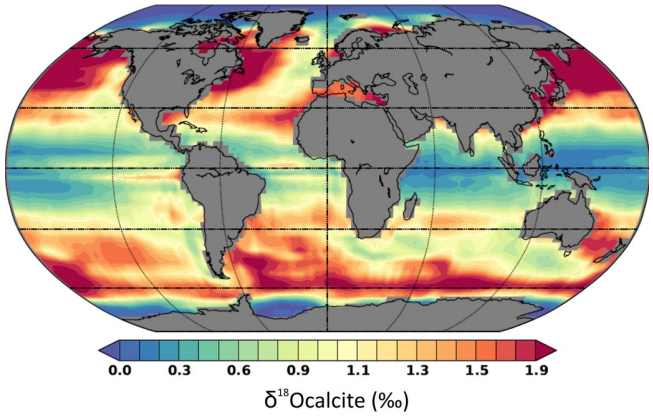

Fig. 7. Simulated seasonal amplitude for ocean calcite δ^{18}O (surface) for present day with *i*LOVECLIM.

dextral (Ottens, 1992; Ostermann et al., 2001; Pak and Kennett, 2002; Pak et al., 2004; Kuroyangi and Kawahata, 2004; von Langen et al., 2005; Came et al., 2007) and 0–150 m for *N. Pachyderma sinistral* (Kohfeld et al., 1996; Bauch, 1997; Bauch et al., 2002; Simstich, 2003) (Table 1). In first approximation, a depth habitat of 0–50 m seems to be suitable to compare the model results with a global and varied dataset. Indeed, for this depth habitat, the relationship between model results and data exhibit a very strong correlation ($R^2 = 0.85$, with a slope of 0.92 and an intercept of 0.15) (Fig. 6). For a depth habitat of 0–20 m, the slope of the relation is 0.89 and the intercept is 0.27, suggesting that the depth habitat is not the main control of the calcite-δ^{18}O signal. We obtain a very good quantitative agreement for calcite δ^{18}O with high-depleted values in the tropical regions (around -3 ‰) and more enriched values in high latitude regions (around 4 ‰), reflecting the combination of both $\delta^{18}O_{sw}$ and temperature changes with latitudes (Fig. 5) (Roche and Caley, 2013).

It is also important to note that both calcite-δ^{18}O and shell flux to the sea floor vary seasonally (Williams et al., 1981; Thunnel et al., 1999). The environmental conditions recorded by the oxygen isotope composition of fossil foraminifera are therefore distorted towards the peak season and highly productive years (Waelbroeck et al., 2005). *G. Ruber pink*, *G. Ruber white*, *G. sacculifer* and *N. Pachyderma sinistral* seems to record a summer signal (Tolderlund and Bé, 1971; Wu and Hillaire-Marcel, 1994; Ganssen and Kroon, 2000; Anand et al., 2003; Waelbroeck et al., 2005; Farmer et al., 2007), whereas *G. bulloides* seems to record a spring/start of summer signal (Ganssen and Kroon, 2000; Pak et al., 2004) and *N. Pachyderma dextral* calcifies throughout the year (Ostermann et al., 2001).

To take into account the seasonal effect we calculate the amplitude in calcite δ^{18}O for the two extreme months in comparison to the mean annual value (Fig. 7). These two end-members represent the extreme configurations in which blooms lead to a 100 % of the carbonate deposit. The range between these two end-members corresponds to all the different possibilities for carbonate deposit. The entire range is from 0–2 ‰ with a weak or null seasonal effect at low and high latitudes, whereas we observe the more pronounced seasonal effect at mid-latitudes. This seasonal range in calcite-δ^{18}O values could explain part of the shift and dispersion observed with the equilibrium 1 : 1 line but correspond to a factor of secondary importance (Fig. 6).

Overall, the model is able to well reproduce the data. This implies that temperature and the isotopic composition of the seawater are the main control on the fossil-δ^{18}O signal recorded in foraminifer's shells at the global scale, when all species are grouped together.

We then realised a data–model comparison for the calcite-δ^{18}O signal for individual species (Fig. 8). For this comparison, the use of palaeotemperature equations derived for living planktonic foraminifera (Mulitza et al., 2003) could be more appropriate than the palaeotemperature equation derived for inorganic precipitates (Shackleton, 1974). We test this possibility but the results indicate no differences for the different equations (Table 1), confirming that over the oceanic temperature range, the slopes of the equations derived for living species agree with the slopes obtained from inorganic precipitates (Mulitza et al., 2003). A significant relationship between data and model results is found for each species except *N. Pachyderma sinistral* (Table 1, Fig. 8). This foraminifer lives at high latitudes, in polar waters. Some caveats in the model for the polar regions as well as complex environmental factors driven by the δ^{18}O signal of this specie are probably responsible for the weak correlation observed (Fig. 8). For example, *N. Pachyderma* has been found to have a secondary calcification phase at depth which can be as much as 75 % of the individual mass (Kohfeld et al., 1996; Schmidt and Mulitza, 2002). Also, the depth habitat of this species has been found to be very variable (Ottens, 1992; Kohfeld et al., 1996; Bauch, 1997; Ostermann et al.,

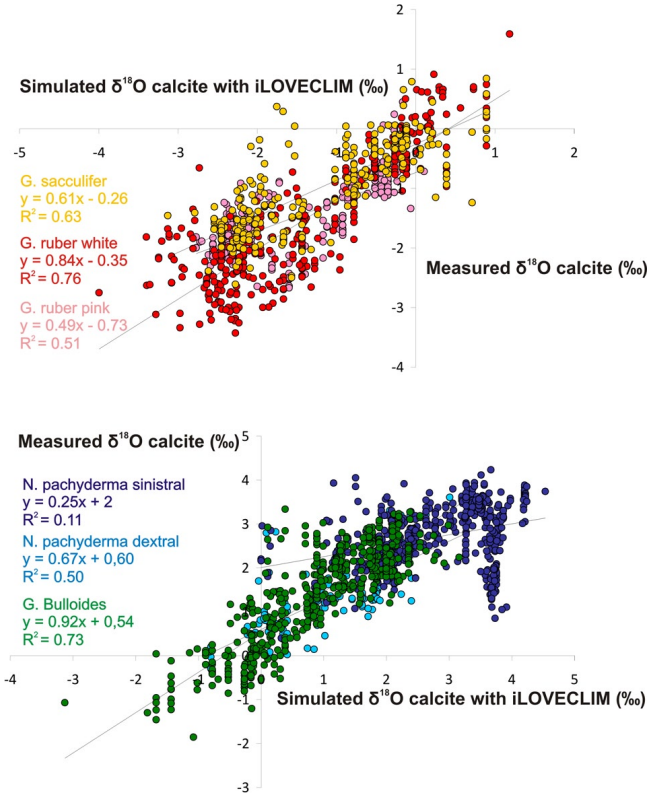

Fig. 8. Relationship between the ocean calcite δ^{18}O calculated in the model (0–25 m for *G. ruber pink*; 0–50 m for *G. ruber white*, *G. sacculifer* and *G. bulloides*; 0–75 m for *N. pachyderma dextral*; 0–150 m for *N. pachyderma sinistral*) and calcite-δ^{18}O measurements for each of the shallowest dwelling foraminifer species (Waelbroeck et al., 2005, extended by 62 points: Table S2).

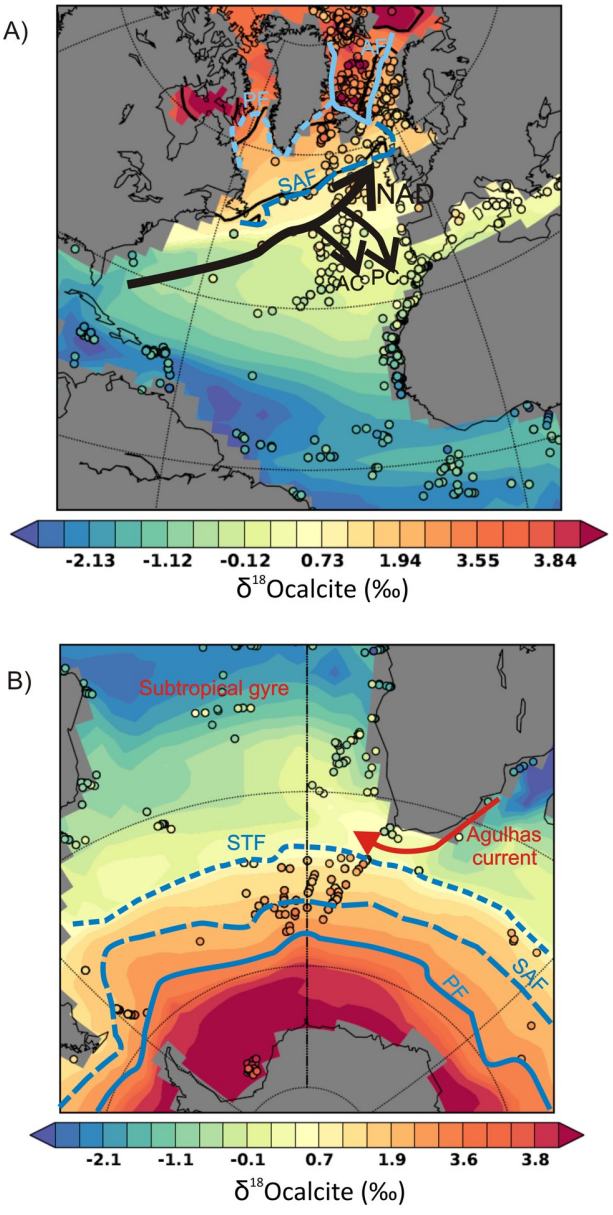

Fig. 9. Regional comparison between simulated ocean calcite δ^{18}O (0–50 m) for the present day with *i*LOVECLIM and calcite-δ^{18}O measurements on the various shallowest dwelling foraminifer species (Waelbroeck et al., 2005, extended by 62 points: Table S2) for **(A)** the North Atlantic Ocean: the North Atlantic Drift (NAD), major boundary return currents (PC, Portugal Current; AC, Azores Current) (Sverdrup et al., 1942; Crowley, 1981; Dickson et al., 1988) and major hydrographic fronts are indicated. Black lines indicate the position of hydrographic fronts as described in the text with the calcite-δ^{18}O signal: PF, polar front (3.94 ‰); AF, Arctic front (2.93 ‰); SAF, sub-Arctic front (1.13 ‰) and blue lines indicate the position described in Dickson et al. (1988). **(B)** The South Atlantic Ocean: major hydrographic fronts are indicated: PF, polar front; SAF, South Antarctic front; STF, sub-tropical front (Peterson and Stramma, 1991). Note that the legend is non-linear.

2001; Bauch et al., 2002; Pak and Kennett, 2002; Simstich, 2003; Pak et al., 2004; Kuroyangi and Kawahata, 2004; von Langen et al., 2005; Came et al., 2007).

We also note that when individual species are considered, the correlation is weaker compared to when species as grouped together (Table 1, Figs. 6 and 8). This probably reflects the stronger influence of species–specific habitat depth, seasonality and other ecological effects (Bemis et al., 1998; Schmidt and Mulitza, 2002; Fraile et al., 2007, 2008). In addition, biases linked to sedimentation and post-deposit effects such as bioturbation or dissolution (Waelbroeck et al., 2005) can also play a role.

To test the ability of the model to represent the data at a regional scale we generated enlargement of the North Atlantic Ocean (Fig. 9a). We investigate the potential of the calcite-δ^{18}O signal to track the main hydrographic conditions in the region. To determine the position of the fronts, we use the actual temperature and salinity changes that characterise these fronts and convert it into calcite-δ^{18}O values. The sub-Arctic Front (SAF) has a high range of variability for temperature and salinity values with a annual mean of around 13 °C

and 35.4 salinity units (s.u), respectively (Belkin and Levitus, 1996 and references therein). Using the actual relationship of Legrande and Schmidt (2006) for the North Atlantic Ocean ($\delta^{18}O = 0.55 \times$ sea surface salinity (SSS)-18.98) and the equation of Shackleton (1974), we obtain a value of 1.13 ‰ for the δ^{18}O calcite. The polar front (PF) is characterised by surface water temperature and salinity lower than 0 °C and 34.4 s.u, respectively (Bauch et al., 1999). Using the actual relationship of Legrande and Schmidt (2006) for the GIN seas ($\delta^{18}O = 0.6 \times$ SSS-20.71), we obtain a value of 3.94 ‰ for the δ^{18}O calcite. The transition between the Atlantic waters and the Arctic domain is through the Arctic front (AF). In this area, the Atlantic inflow of water has salinity above 35 s.u and a temperature of 5 °C (Skagseth et al., 2008) leading to a δ^{18}O calcite value of 2.93‰. These different values of δ^{18}O calcite track faithfully the actual position of the front as described in Dickson et al. (1988) and are well documented by our data–model comparison results (Fig. 9a).

Similarly, the main hydrographic conditions in the South Atlantic Ocean with the hydrographic fronts are well documented by the calcite-δ^{18}O signal (Fig. 9b). The STF is best defined by salinity (the 34.81 s.u halocline in this area) (Edwards and Emery, 1982) or the 11 °C isotherm at 100 m depth. Using the actual relationship of Legrande and Schmidt (2006) for the South Atlantic Ocean ($\delta^{18}O = 0.51 \times$ SSS-17.4) and the equation of Shackleton (1974), we obtain a value of 0.77‰ for the δ^{18}O calcite. For the SAF, we use the definition of the isotherm 4 °C near 200 m depth, and a salinity of 34.5 s.u south of the front (Peterson and Stramma, 1991). Using the actual relationship of Legrande and Schmidt (2006) for the Austral Ocean ($\delta^{18}O = 0.24 \times$ SSS-8.45), we can calculate a δ^{18}O calcite value of 2.65‰. For the polar front (PF), the definition relies only on the isotherm and not to salinity. Nowlin et al. (1977) used the northern extent of the 0 °C isotherm. We also use a mean value of -0.4‰ for the $\delta^{18}O_{sw}$ of the Austral Ocean (Legrande and Schmidt, 2006) leading to a value of 3.6 ‰ for δ^{18}O calcite. These different values of δ^{18}O calcite track well the actual position of the front as described in Peterson and Stramma (1991) (Fig. 9b).

Applying this data–model comparison for calcite δ^{18}O in past climates could constitute an interesting tool for mapping the potential shifts of the frontal systems and circulation changes through time, assuming that changes in foraminiferal habitat depth (Telford et al., 2013) and salinity–temperature relationship in oceanic fronts stay relatively stable with time. Previous data studies on the amplitude of the calcite δ^{18}O have documented hydrographic changes during the 8.2 kyr event, the Younger Dryas event, Heinrich events and the Last Glacial Maximum (LGM) (Cortijo et al., 2005; Eynaud et al., 2009).

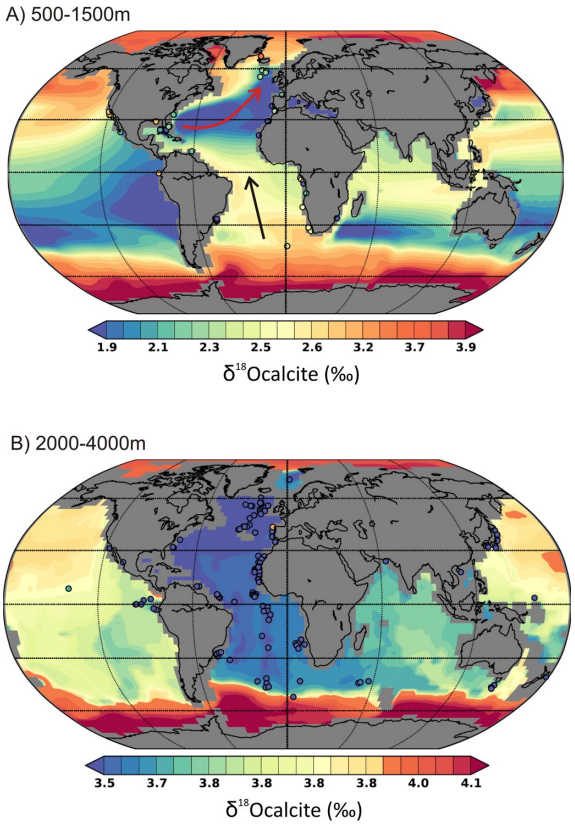

Fig. 10. Simulated ocean calcite δ^{18}O (500–1500 m in **(A)** and 2000–4000 m in **(B)**) for the present day with *i*LOVECLIM. Superimposed dots represent calcite-δ^{18}O data measured on benthic foraminifer species (Marchal and Curry, 2008, extended by 73 points: Table S2). The North Atlantic drift (red arrow in **A**) is well represented as the penetration of the Antarctic intermediate waters moving northward (black arrow in **A**). Note that the legend is non-linear.

3.2.2 Intermediate and deep ocean

Since we obtain very good results at the surface of the ocean it is interesting to investigate intermediate and deep ocean results in comparison to available data of benthic foraminifers. To document the intermediate depth circulation, we present in Fig. 10a the ocean calcite δ^{18}O for a mean depth of 500–1500 m. A good agreement is observed between model results and data. The North Atlantic drift is well represented and the penetration of the Antarctic intermediate waters moving northward is also visible. Any potential changes in these oceanic circulation systems in the past could be documented by a data–model comparison exercise. Outside of the Atlantic Ocean region, the data are too sparse to validate the model results. Supplementary data in the Indian Ocean, Pacific Ocean and Southern Ocean would be a major advance in order to validate the observed distribution in calcite δ^{18}O at intermediate depth.

Concerning the mean deep ocean (2000–4000 m), Fig. 10b indicates a relatively good agreement between model results

and data for the Atlantic Ocean contrary to the other parts of the world ocean. Nonetheless, the calcite δ^{18}O simulated with *i*LOVECLIM for the deep ocean is globally too high in comparison to data. The values in the model are actually close to values reached between interglacial and glacial periods (3.8–4.2 ‰). After investigation, it appears that two factors can explain this abnormally high δ^{18}O signal. First the modelled distribution of $\delta^{18}O_{sw}$ is 0.25 per mil lower than data between 20° S and 30° N (Roche and Caley, 2013). Second, the modelled temperature of deep water is around 2 °C lower than data, a pattern particularly marked in the Austral Ocean. The caveat for the deep ocean temperature with the model is unclear so far and would be the matter of future investigation. We hypothesise that it is linked to the deep water formation in the Southern Ocean since it shows a marked underestimation in that region. Together, these two biases explain the high δ^{18}O calcite signal in the model. These results also elegantly suggest that changes in the deep water temperature by only few degrees can have an important effect of the benthic δ^{18}O calcite signal, a pattern that requires further investigation during past climate changes.

4 Conclusions

Concerning the atmospheric component and contrary to the δ^{18}O in precipitation, the limitation of the model together with the processes operating in the atmosphere, soil zone, epikarst and cave system hamper a good quantitative data–model comparison for the calcite-δ^{18}O signal. It remains to be tested whether the use of more complex isotope-enabled models at higher resolution added to the inclusion of supplementary processes operating between the atmosphere and the cave system would allow to obtain better results. It is necessary to assess such improvements in parallel with improvements regarding the potential biases occurring in the natural environment and affecting the measured calcite-δ^{18}O signal. It also remains to be tested if qualitative data – model comparison for the calcite-δ^{18}O signal (i.e. anomaly between the past and present day) would give better results. Based on our work and for simplicity reasons, it appears that reconstructed fossil water isotopic signals by fluid inclusions in speleothems is a more promising way to compare quantitative simulation results with climate data, a comparison which is today restricted to ice core records. The relationship between the δ^{18}O in precipitation and climate variables such as temperature and precipitation rates could be investigated for past time periods.

Concerning the oceanic component, the simulated calcite δ^{18}O compare quantitatively well with global late Holocene planktonic foraminifer δ^{18}O data. Our results indicate that temperature and the isotopic composition of the seawater are the main control on the fossil-δ^{18}O signal recorded in foraminifer's shells at the global and regional scale. Nonetheless, depth life, seasonality and other ecological effects play also a role and are more expressed when individual species are considered. Further works with more sophisticated ecological models are needed to refine these conclusions and increase the quantitative match of the modelled calcite-δ^{18}O results with data. We argue that a data–model comparison exercise for calcite δ^{18}O in past climate could constitute an interesting tool for mapping the potential shifts of the frontal systems and circulation changes throughout time. Of particular interest is the ocean circulation at the LGM. By simulating both the calcite δ^{18}O and $\delta^{18}O_{sw}$ in the model and by comparison with foraminifer's calcite-δ^{18}O data it would be possible to address the LGM tropical sea surface temperature controversy (large east–west gradients)(MARGO Project Members, 2009).

Similarly to surface ocean, the potential changes in intermediate oceanic circulation systems in the past could be documented by a data–model comparison exercise but an extension of the spatial data coverage is necessary. For deep ocean calcite-δ^{18}O signal, the abnormally low-modelled deep ocean temperature would be the matter of future investigation in order to quantitatively compare the results with data.

Supplementary material related to this article is available online at: http://www.geosci-model-dev.net/6/1505/2013/gmd-6-1505-2013-supplement.pdf.

Acknowledgements. T. Caley is supported by NWO through the VIDI/AC^{2}ME project no 864.09.013. D. M. Roche is supported by NWO through the VIDI/AC^{2}ME project no 864.09.013 and by CNRS-INSU. The authors wish to thank D. Genty for useful discussion on equilibrium conditions during speleothem calcite growth. Institut Pierre Simon Laplace is gratefully acknowledged for hosting the iLOVECLIM model code under the LUDUS framework project (https://forge.ipsl.jussieu.fr/ludus). This is NWO/AC^{2}ME contribution number 03.

Edited by: R. Marsh

References

Anand, P., Elderfield, H., and Conte, M. H.: Calibration of Mg/Ca thermometry in planktonic foraminifera from a sediment trap time series, Paleoceanography, 18, 1050, doi:10.1029/2002PA000846, 2003.

Baertschi, P.: Absolute ^{18}O content of Standard Mean Ocean Water, Earth Planet. Sci. Lett., 31, 341–344, 1976.

Bauch, D.: Oxygen isotope composition of living Neogloboquadrina pachyderma (sin.) in the Arctic Ocean, Earth Planet. Sci. Lett., 146, 47–58, 1997.

Bauch, H. A., Erlenkeuser, H., Fahl, K., Spielhagen, R. F., Weinelt, M. S., Andruleit, H., and Heinrich, R.: Evidence for a steeper Eemian than Holocene sea surface temperature gradient between Arctic and sub-Arctic regions, Palaeogeogr. Palaeoclim., 144, 95–117, 1999.

Bauch, D., Erlenkeuser, H., Winckler, G., Pavlova, G., and Thiede, J.: Carbon isotopes and habitat of polar planktic foraminifera in

the Okhotsk Sea: The "carbonate ion effect" under natural conditions, Mar. Micropaleontol., 45, 83–99, 2002.

Belkin, I. M. and Levitus, S.: Temporal variability of the Subarctic Front near the Charlie-Gibbs Fracture Zone, J. Geophys. Res., 101, 28317–28324, 1996.

Bemis, B. E., Spero, H. J., Bijma, J., and Lea, D. W.: Reevaluation of the oxygen isotopic composition of planktonic foraminifera: experimental results and revised paleotemperature equations, Paleoceanography, 13, 150–160, 1998.

Burns, S. J., Fleitmann, D., Mudelsee, M., Neff, U., Matter, A., and Mangini, A.: A 780-year annually resolved record of Indian Ocean monsoon precipitation from a speleothem from South Oman, J. Geophys. Res. Atmos., 107, 4434, doi:10.1029/2001JD001281, 2002.

Came, R. E., Oppo, D. W., and McManus, J. F.: Amplitude and timing of temperature and salinity variability in the subpolar North Atlantic over the past 10 k.y, Geology, 35, 315–318, 2007.

Coplen, T. B.: Editorial: more uncertainty than necessary, Paleoceanography 11, 369–370, 1996.

Coplen, T. B., Kendall, C., and Hopple, J.: Comparison of stable isotope reference samples, Nature, 302, 236–238, 1983.

Cortijo, E., Duplessy, J., Labeyrie, L., Duprat, J., and Paillard, D.: Heinrich events: Hydrological impact, C. R. Geosci., 337, 897–907, doi:10.1016/j.crte.2005.04.011, 2005.

Craig, H.: Isotopic standards for carbon and oxygen and correction factors for mass-spectrometric analysis of carbon dioxide, Geochim. Cosmochim. Acta, 12, 133–149, 1957.

Craig, H. and Gordon, L. I.: Deuterium and oxygen 18 variations in the ocean and the marine atmosphere, in: Stable Isotopes in Oceanographic Studies and Paleotemperatures, edited by: Tongiorgi, E., Consiglio nazionale delle ricerche, Spoleto, 9–122, 1965.

Crowley, T.: Temperature and circulation changes in the eastern north Atlantic during the last 150,000 years: Evidence from the planktonic foraminiferal record, Mar. Micropaleontol., 6, 97–129, 1981.

Daëron, M., Guo, W., Eiler, J., Genty, D., Blamart, D., Boch, R., Drysdale, R., Maire, K., Wainer, G., and Zanchetta, G.: $^{13}C^{18}O$ clumping in speleothems: observations from natural caves and precipitation experiments, Geochim. Cosmochim. Acta, 75, 3303–3317, 2011.

Dansgaard, W.: The abundance of ^{18}O in atmospheric water and water vapour, Tellus, 5, 461–469, 1953.

Dansgaard, W.: Stable isotopes in precipitation, Tellus, 16, 436–468, 1964.

Delaygue, G., Jouzel, J., and Dutay, J. C.: Oxygen 18-salinity relationship simulated by an oceanic general circulation model, Earth Planet. Sci. Lett., 178, 113–123, doi:10.1016/S0012-821X(00)00073-X, 2000.

Dickson, R. R., Meincke, J., Malmberg, S. A., and Lee, A. J.: The "great salinity anomaly" in the northern North Atlantic 1968–1982, Prog. Oceanogr., 20, 103–151, doi:10.1016/0079-6611(88)90049-3, 1988.

Edwards, R. J. and Emery, W. J.: Australasian southern ocean frontal structure during summer 1976–77, Austr. J. Mar. Freshw. Res., 33, 3–22, 1982.

Eynaud, F., de Abreu, L., Voelker, A., Schönfeld, J., Salgueiro, E., Turon, J. L., Penaud, A., Toucanne, S., Naughton, F., Sanchez-Goñi, M. F., Malaizé, B., and Cacho, I.: Position of the Polar Front along the western Iberian margin during key cold episodes of the last 45 ka, Geochem. Geophys. Geosys., 10, Q07U05, doi:10.1029/2009GC002398, 2009.

Farmer, E. C., Kaplan, A., de Menocal, P. B., and Lynch-Stieglitz, J.: Corroborating ecological depth preferences of planktonic foraminifera in the tropical Atlantic with the stable oxygen isotope ratios of core top specimens, Paleoceanography 22, PA3205, doi:10.1029/2006PA001361, 2007.

Fraile, I., Schulz, M., Mulitza, S., and Kucera, M.: A dynamic global model for planktonic foraminifera, Biogeosciences Discuss., 4, 4323–4384, doi:10.5194/bgd-4-4323-2007, 2007.

Fraile, I., Schulz, M., Mulitza, S., and Kucera, M.: Predicting the global distribution of planktonic foraminifera using a dynamic ecosystem model, Biogeosciences, 5, 891–911, doi:10.5194/bg-5-891-2008, 2008.

Fleitmann, D., Burns, S. J., Mudelsee, M., Neff, U., Kramers, J., Mangini, A., and Matter, A.: Holocene forcing of the Indian monsoon recorded in a stalagmite from southern Oman, Science, 300, 1737–1739, 2003.

Ganssen, G. M. and Kroon, D.: The isotopic signature of planktonic foraminifera from NE Atlantic surface sediments: implications for the reconstruction of past oceanic conditions, J. Geol. Soc., 157, 693–699, 2000.

Goosse, H., Brovkin, V., Fichefet, T., Haarsma, R., Huybrechts, P., Jongma, J., Mouchet, A., Selten, F., Barriat, P.-Y., Campin, J.-M., Deleersnijder, E., Driesschaert, E., Goelzer, H., Janssens, I., Loutre, M.-F., Morales Maqueda, M. A., Opsteegh, T., Mathieu, P.-P., Munhoven, G., Pettersson, E. J., Renssen, H., Roche, D. M., Schaeffer, M., Tartinville, B., Timmermann, A., and Weber, S. L.: Description of the Earth system model of intermediate complexity LOVECLIM version 1.2, Geosci. Model Dev., 3, 603–633, doi:10.5194/gmd-3-603-2010, 2010.

Hendy, C. H.: The isotopic geochemistry of speleothems. 1. The calculation of the effects of different modes of formation on the isotopic composition of speleothems and their applicability as paleoclimatic indicators, Geochim. Cosmochim. Acta, 35, 801–824, 1971.

Hoffmann, G., Werner, M., and Heimann, M.: Water isotope module of the ECHAM atmospheric general circulation model: A study on timescales from days to several years, J. Geophys. Res., 103, 16871–16896, 1998.

Hoffmann, G., Ramirez, E., Taupin, J. D., Francou, B., Ribstein, P., Delmas, R., Dürr, H., Gallaire, R., Simões, J., Schotterer, U., Stievenard, M., and Werner, M.: Coherent isotope history of Andean ice cores over the last century, Geophys. Res. Lett., 30, 1179, doi:10.1029/2002GL014870, 2003.

Hut, G.: Stable Isotope Reference Samples for Geochemical and Hydrological Investigations. Consultant Group Meeting IAEA, Vienna 16–18 September 1985, Report to the Director General, International Atomic Energy Agency, Vienna, 1987.

Jacobs, S. S., Fairbanks, R. G., and Horibe, Y.: Origin and evolution of water masses near the Antarctic continental margin: Evidence from $H_2{}^{18}O/H_2{}^{16}O$ ratios in seawater, in: Oceanology of the Antarctic Continental Shelf, edited by: Jacobs, S. S., Antarct. Res. Ser., 43, 59–85, AGU, Washington, DC, 1985.

Joussaume, S. and Jouzel, J.: Paleoclimatic tracers: An investigation using an atmospheric general circulation model under ice age conditions: 2. Water isotopes, J. Geophys. Res., 98, 2807–2830, 1993.

Jouzel, J.: Water stable isotopes: Atmospheric composition and applications in polar ice core studies, Treatise Geochem., 4, 213–243, 2003.

Jouzel, J., Koster, R. D., Suozzo, R. J., Russel, G. L., White, J. W. C., and Broecker, W. S.: Simulations of the HDO and $H_2{}^{18}O$ atmospheric cycles using the NASA GISS General Circulation Model: The seasonal cycle for present-day conditions, J. Geophys. Res., 92, 14739–14760, 1987.

Jouzel, J., Masson-Delmotte, V., Cattani, O., Dreyfus, G., Falourd, S., Hoffmann, G., Minster, B., Nouet, J., Barnola, J. M., Chappellaz, J., Fischer, H., Gallet, J. C., Johnsen, S., Leuenberger, M., Loulergue, L., Luethi, D., Oerter, H., Parrenin, F., Raisbeck, G., Raynaud, D., Schilt, S., Schwander, J., Selmo, E., Souchez, R., Spahni, R., Stauffer, B., Steffensen, J. P., Stenni, B., Stocker, T. F., Tison, J. L., Werner, M., and Wolff, E. W.: Orbital and Millennial Antarctic Climate Variability over the Past 800,000 Years, Science, 317, 793–796, 2007.

Kim, S.-T. and O'Neil, J. R.: Equilibrium and nonequilibrium oxygen isotope effects in synthetic carbonates, Geochim. Cosmochim. Acta, 61, 3461–3475, 1997.

Kohfeld, K. E., Fairbanks, R. G., Smith, S. L., and Walsh, I. D.: Neogloboquadrina pachyderma (sinistral coiling) as paleoceanographic tracers in polar oceans: Evidence from Northeast Water Polynya plankton tows, sediment traps, and surface sediments, Paleoceanography, 11, 679–699, 1996.

Kuroyanagi, A. and Kawahata, H.: Vertical distribution of living planktonic foraminifera in the seas around Japan, Marine Micropaleont., 53, 173–196, 2004.

Lachniet, M. S.: Climatic and environmental controls on speleothem oxygen isotope values, Quatern. Sci. Rev., 28, 412–432, 2009.

Lee, J.-E., Fung, I., DePaolo, D., and Fennig, C. C.: Analysis of the global distribution of water isotopes using the NCAR atmospheric general circulation model, J. Geophys. Res., 112, D16306, doi:10.1029/2006JD007657, 2007.

LeGrande, A. N. and Schmidt, G. A.: Global gridded dataset of the oxygen isotopic composition in seawater, Geophys. Res. Lett., 33, L12604, doi:10.1029/2006GL026011, 2006.

LeGrande, A. N. and Schmidt, G. A.: Sources of Holocene variability of oxygen isotopes in paleoclimate archives, Clim. Past, 5, 441–455, doi:10.5194/cp-5-441-2009, 2009.

LeGrande, A. N. and Schmidt, G. A.: Water isotopologues as a Quantitative Paleosalinity Proxy, Paleoceanography, 26, PA3225, doi:10.1029/2010PA002043, 2011.

Leng, M. J. and Marshall, J. D.: Palaeoclimate interpretation of stable isotope data from lake sediment archives, Quaternary Sci. Rev., 23, 811–831, 2004.

Levitus, S. and Boyer, T. P.: World Ocean Atlas 1994 Volume 4: Temperature, number 4, 1994.

Marchal, O. and Curry, W. B.: On the abyssal circulation in the glacial Atlantic, J. Phys. Oceanogr., 38, 2014–2037, doi:10.1175/2008JPO3895.1, 2008.

MARGO Project Members, Waelbroeck, C., Paul, A., Kucera, M., Rosell-Melee, A., Weinelt, M., Schneider, R., Mix, A.C., Abelmann, A., Armand, L., Bard, E., Barker, S., Barrows, T. T., Benway, H., Cacho, I., Chen, M. T., Cortijo, E., Crosta, X., de Vernal, A., Dokken, T., Duprat, J., Elderfield, H., Eynaud, F., Gersonde, R., Hayes, A., Henry, M., Hillaire-Marcel, C., Huang, C. C., Jansen, E., Juggins, S., Kallel, N., Kiefer, T., Kienast, M., Labeyrie, L., Leclaire, H., Londeix, L., Mangin, S., Matthiessen, J., Marret, F., Meland, M., Morey, A. E., Mulitza, S., Pfaumann, U., Pisias, N. G., Radi, T., Rochon, A., Rohling, E. J., Sbaf, L., Schafer-Neth, C., Solignac, S., Spero, H., Tachikawa, K., and Turon, J. L.: Constraints on the magnitude and patterns of ocean cooling at the Last Glacial Maximum, Nat. Geosci., 2, 127–132, 2009.

Mathieu, R., Pollard, D., Cole, J., White, J. W. C., Webb, R. S., and Thompson, S. L.: Simulation of stable water isotope variations by the GENESIS GCM for modern conditions, J. Geophys. Res., 107, 4037, doi:10.1029/2001JD900255, 2002.

Mickler, P., Stern, L., and Banner, J.: Large kinetic isotope effects in modern speleothems, Geol. Soc. Am. Bull., 118, 65–81. doi:10.1130/B25698.1, 2006.

Mulitza, S., Boltovskoy, D., Donner, B., Meggers, H., Paul, A., and Wefer, G.: Temperature: δ18O relationships of planktonic foraminifera collected from surface waters, Palaeogeogr. Palaeoclim., 202, 143–152, 2003.

Noone, D. and Simmonds, I.: Associations between δ^{18}O of water and climate parameters in a simulation of atmospheric circulation for 1979–95, J. Climate, 15, 3150–3169, 2002.

Nowlin, W. D., Whitworth III, T., and Pillsbury, R. D.: Structure and transport of the Antarctic Circumpolar Current at Drake Passage from short-term measurements, J. Phys. Oceanogr., 7, 788–802, 1977.

Ostermann, D. R., Olafsson, J., Manganini, S., Curry, W. B., and Honjo, S.: A dramatic increase in particle flux in the Iceland Sea since 1997, results from a 15-year time series, in: International Conference on Paleoceanography, 7th, Program and Abstracts: Sapporo, Japan, Hokkaido University, 169 pp., 2001.

Ottens, J. J.: Planktic foraminifera as indicators of ocean environments in the northeast Atlantic [Ph.D. thesis]: Amsterdam, Vrije Universiteit Amsterdam, 189 pp., 1992.

Pak, D. K. and Kennett, J. P.: A foraminiferal proxy for upper water mass stratification, J. Foraminiferal Res., 32, 319–327, 2002.

Pak, D. K., Lea, D. W., and Kennett, J. P.: Seasonal and interannual variation in Santa Barbara Basin water temperatures observed in sediment trap foraminiferal Mg/Ca, Geochem. Geophys. Geosyst., 5, Q12008, doi:10.1029/2004GC000760, 2004.

Paul, A., Mulitza, S., Patzold, J., and Wolff, T.: Simulation of oxygen isotopes in a global ocean model, in: Use of Proxies in Paleoceanography: Examples From the South Atlantic, edited by: Fischer, G. and Wefer, G., Springer, New York, 655–686, 1999.

Peterson, R. G. and Stramma, L.: Upper-level circulation in the South Atlantic Ocean, Prog. Oceanogr., 26, 1–73, 1991.

Risi, C., Bony, S., Vimeux, F., and Jouzel, J.: Water stable isotopes in the LMDZ4 general circulation model: Model evaluation for present day and past climates and applications to climatic interpretation of tropical isotopic records, J. Geophys. Res. 115, D12118, doi:10.1029/2009JD013255, 2010.

Roche, D. M.: δ^{18}O water isotope in the *i*LOVECLIM model (version 1.0) – Part 1: Implementation and verification, Geosci. Model Dev., 6, 1481–1491, doi:10.5194/gmd-6-1481-2013, 2013.

Roche, D. M. and Caley, T.: δ^{18}O water isotope in the *i*LOVECLIM model (version 1.0) – Part 2: Evaluation of model results against observed δ^{18}O in water samples, Geosci. Model Dev., 6, 1493–1504, doi:10.5194/gmd-6-1493-2013, 2013.

Rozanski, K., Araguas-Araguas, L., and Gonfiantini, R.: Isotopic patterns in modern global precipitation, in: Climate Change in Continental Isotopic Records, edited by: Swart, P. K., Geophys. Monogr. Ser., vol. 78, 1–36, AGU, Washington, DC, 1993.

Schmidt, G. A.: Oxygen-18 variations in a global ocean model, Geophys. Res. Lett., 25, 1201–1204, 1998.

Schmidt, G. A. and Mulitza, S.: Global calibration of ecological models for planktic foraminifera from coretop carbonate oxygen-18, Marine Micropaleon., 44, 125–140, 2002.

Schmidt, G. A., LeGrande, A. N., and Hoffmann, G.: Water isotope expressions of intrinsic and forced variability in a coupled ocean-atmosphere model, J. Geophys. Res., 112, D10103, doi:10.1029/2006JD007781, 2007.

Shackleton, N. J.: Attainment of isotopic equilibrium between ocean water and benthonic foraminifera genus Uvigerina: isotopic changes in the ocean during the last glacial, Les méthodes quantitatives d'étude des variations du climat au cours du Pleistocène, Gif-sur-Yvette, Colloque international du CNRS 219, 203–210, 1974.

Sharp, Z.: Principles of Stable Isotope Geochemistry, Pearson Prentice Hall, Upper Saddle River, NJ, 2007.

Simstich, J., Sarnthein, M., and Erlenkeuser, H.: Paired δ^{18}O signals of Neogloboquadrina pachyderma (s) and Turborotalita quinqueloba show thermal stratification structure in Nordic Seas, Marine Micropaleon., 48, 107–125, 2003.

Skagseth, Ø., Furevik, T., Ingvaldsen, R., Loeng, H., Mork, K., Orvik, K., and Ozhigin, V.: Volume and heat transport to the Arctic Ocean via the Norwegian and Barents Seas, in Arctic-Subarctic Ocean Fluxes, edited by: Dickson, R., Meincke, J., and Rhines, P., 45–64, Springer, New York, 2008.

Skinner, L. C., Shackleton, N. J., and Elderfield, H.: Millennial-scale variability of deep-water temperature and delta $\delta^{18}O_{dw}$ indicating deepwater source variations in the Northeast Atlantic, 0–34 cal. ka BP, Geochem. Geophys. Geosyst., 4, 1098, doi:10.1029/2003GC000585, 2003.

Stuiver, M.: Oxygen and carbon isotope ratios of fresh-water carbonates as climatic indicators, J. Geophys. Res., 75, 5247–5257, 1970.

Sturm, C., Zhang, Q., and Noone, D.: An introduction to stable water isotopes in climate models: benefits of forward proxy modelling for paleoclimatology, Clim. Past, 6, 115–129, doi:10.5194/cp-6-115-2010, 2010.

Sverdrup, H. U., Johnson, M. W., and Fleming, R. W.: The Oceans: Their Physics, Chemistry and General Biology, 1060 pp., Prentice-Hall, Englewood, N. J., 1942.

Telford, R. J., Li, C., and Kucera, M.: Mismatch between the depth habitat of planktonic foraminifera and the calibration depth of SST transfer functions may bias reconstructions, Clim. Past, 9, 859–870, doi:10.5194/cp-9-859-2013, 2013.

Thunnel, R., Tappa, E., Pride, C., Kincaid, E.: Sea-surface temperature anomalies associated with the 1997–1998 El Nino recorded in the oxygen isotope composition of planktonic foraminifera, Geology, 27, 843–846, 1999.

Thompson, L. G., Mosley-Thompson, E., and Henderson, K. A.: Ice-core paleoclimate records in tropical South America since the Last Glacial Maximum, J. Quaternary Sci., 15, 1579–1600, 2000.

Tindall, J. C., Valdes, P., and Sime, L. C.: Stable water isotopes in HadCM3: Isotopic signature of El Niño–Southern Oscillation and the tropical amount effect, J. Geophys. Res., 114, D04111, doi:10.1029/2008JD010825, 2009.

Tolderlund, D. S. and Bé, A. W. H.: Seasonal distribution of planktonic foraminifera in the western North Atlantic, Micropaleontology, 17, 297–329, 1971.

Urey, H. C.: Thermodynamic properties of isotopic substances, J. Chem. Soc., 562–581, 1947.

van Breukelen, M. R., Vonhof, H. B., Hellstrom, J. C., Wester, W. C. G., and Kroon, D.: Fossil dripwater in stalagmites reveals Holocene temperature and rainfall variation in Amazonia, Earth Planet. Sci. Lett., 275, 54–60, 2008.

Vimeux, F., Gallaire, R., Bony, S., Hoffmann, G., and Chiang, J. C. H.: What are the climate controls on δD in precipitation in the Zongo Valley (Bolivia)? Implications for the Illimani ice core interpretation, Earth Planet. Sci. Lett., 240, 205–220, 2005.

Vonhof, H. B., van Breukelen, M. R., Postma, O., Rowe, P. J., Atkinson, T. C., and Kroon, D.: A continuous-flow crushing device for on-line d2H analysis of fluid inclusion water in speleothems, Rapid Commun. Mass Spectrom., 20, 2553–2558, 2006.

von Langen, P. J., Pak, D. K., Spero, H. J., and Lea, D. W.: Effects of temperature on Mg/Ca in neogloboquadrinid shells determined by live culturing, Geochem. Geophys. Geosyst., 6, Q10P03, doi:10.1029/2005GC000989, 2005.

Wackerbarth, A., Langebroek, P. M., Werner, M., Lohmann, G., Riechelmann, S., Borsato, A., and Mangini, A.: Simulated oxygen isotopes in cave drip water and speleothem calcite in European caves, Clim. Past, 8, 1781–1799, doi:10.5194/cp-8-1781-2012, 2012.

Waelbroeck, C., Mulitza, S., Spero, H., Dokken, T., Kiefer, T., and Cortijo, E.: A global compilation of Late Holocene planktonic foraminiferal δ^{18}O: Relationship between surface water temperature and δ^{18}O, Quaternary Sci. Rev., 24, 853–878, 2005.

Wang, Y. J., Cheng, H., Edwards, R. L., An, Z. S., Wu, J. Y., Shen, C. C., and Dorale, J. A.: A high-resolution absolute-dated Late Pleistocene monsoon record from Hulu Cave, China, Science, 294, 2345–2348, 2001.

Werner, M., Langebroek, P. M., Carlsen, T., Herold, M., and Lohmann, G.: Stable water isotopes in the ECHAM5 general circulation model: Toward high-resolution isotope modeling on global scale, J. Geophys. Res., 116, D15109, doi:10.1029/2011JD015681, 2011.

Williams, D. F., Bé, A. W., and Fairbanks, R. G.: Seasonal stable isotopic variations in living planktonic foraminifera from Bermuda plankton tows, Palaeogeography, Palaeoclimatology, Palaeoecology, 33, 71–102, 1981.

Wu, G.-P. and Hillaire-Marcel, C.: Oxygen isotope compositions of sinistral Neogloboquadrina pachyderma tests in surface sediments: North Atlantic Ocean, Geochim. Cosmochim. Acta, 58, 1303–1312, 1994.

Xu, X., Werner, M., Butzin, M., and Lohmann, G.: Water isotope variations in the global ocean model MPI-OM, Geosci. Model Dev., 5, 809–818, doi:10.5194/gmd-5-809-2012, 2012.

Yoshimura, K., Kanamitsu, M., Noone, D., and Oki, T.: Historical isotope simulation using reanalysis atmospheric data, J. Geophys. Res., 113, D19108, doi:10.1029/2008JD010074, 2008.

Zhou, J., Poulsen, C. J., Pollard, D., and White, T. S.: Simulation of modern and middle Cretaceous marine δ^{18}O with an ocean-atmosphere general circulation model, Paleoceanography, 23, PA3223, doi:10.1029/2008PA001596, 2008.